

## DYNAMICAL MODELING OF NEARBY GALAXIES

M. JOVANOVIĆ<sup>1</sup>, S. SAMUROVIĆ<sup>1</sup>, M. M. ĆIRKOVIĆ<sup>1,2</sup> and A. VUDRAGOVIĆ<sup>1</sup>

<sup>1</sup>*Astronomical Observatory, Volgina 7, 11000 Belgrade, Serbia*  
*E-mail: milena@aob.rs*

<sup>2</sup>*Future of Humanity Institute, Faculty of Philosophy, University of Oxford,*  
*Suite 8, Littlegate House, 16/17 St Ebbe's Street, Oxford, OX1 1PT, UK*

**Abstract.** Here we present the procedure of detailed dynamical modeling applied on a sample of galaxies based on THINGS (The HI Nearby Galaxy Survey). Stellar mass is derived for all galaxies using a free mass-to-light ratio. Where possible, a modeling procedure is also done for a fixed  $M/L^*$  based on modern stellar population models. Finally we give the outline of the ongoing work, which is determining the baryon distribution of the Milky Way environment reflected by the Baryonic Mass Function based on the same sample of galaxies.

### 1. INTRODUCTION

Dynamical modeling of a galaxy recovers the total mass that interacts gravitationally: stellar, gaseous, dark matter. The mass of a galaxy, although not the sole driver of its evolution as it almost is in stars, is still very important for the processes of galaxy formation and evolution; a galaxy's mass probably modulates crucial evolution processes like star formation and quenching (e.g. Courteau et al. 2014). We observe the dynamical mass through the motions of test-particles inside of the gravitational potential of that mass.

In our work, the test-particle or tracer of the gravitational field is HI gas. Therefore, we are interested in galaxies rich with cold neutral gas. Rotationally supported objects are required for this analysis because in that case rotational velocity at a certain radius equals the circular velocity in the disk. Then the virial theorem reduces nicely to the simple expression:

$$V_{\text{circ}}^2(r) = r \frac{d\phi}{dr} = G \frac{M(r)}{r} \quad (1)$$

All of this is done within the framework of Newtonian/Einstein gravity.

## 2. SAMPLE

The sample we used is derived from the THINGS<sup>1</sup> (The HI Nearby Galaxy Survey) survey conducted on the VLA telescope, which is described in Walter et al. (2008) and analyzed in a similar manner in de Blok et al. (2008). The sample covers nearby galaxies ( $z < 0.003$ ,  $D < 15$  Mpc) with a large span of morphologies, masses and sizes. Obviously, it was an HI-selected sample and no early-type or lenticular galaxies were represented. From the total of 34 observed objects only (up to) 20 were usable for deriving rotation curves by satisfying the criteria of rotationally-dominated kinematics, not undergoing disruptive interactions and having favorable geometry (inclination between  $45 - 70^\circ$ ).

## 3. METHOD

### 3.1. ROTATION CURVE

The rotation curve for these types of very detailed radio observations can be derived through forming a two-dimensional velocity field. We formed the velocity field from the standard three-dimensional data cube by fitting of a (in most cases) Gauss-Hermite polynomial to the HI line in every spatial point of the observed galaxy disk (see Fig. 1, left). In two cases, for the galaxies NGC 2366 and IC 2574, there were other significant types of motion other than rotation. For them we derived a procedure to extract what we call the 'rotationally dominated velocity field'. The developed procedure is based on the one described in Oh et al. (2008) but simplified, while remaining robust. The schematic of the data cube and determination of the center of the line is shown in Fig. 1 on the left. On the right of the Fig. 1 we show the subsequently constructed velocity field from all the determined line centers in the case of the galaxy NGC 2841 (Samurović, Vudragović & Jovanović 2015).

The rotation curve is derived by tilted-ring fitting to the constructed velocity field through varying parameters in the following expression:

$$V(x, y) = V_{\text{sys}} + V_c(r) \sin i \cos \theta (+V_{\text{exp}}). \quad (2)$$

Here  $V(x, y)$  is the resulting velocity on the projected point of the galaxy's disk,  $V_{\text{sys}}$  is systemic velocity,  $V_c(r)$  is the circular or rotation velocity at a given radius  $r$ ,  $i$  is the inclination,  $\theta$  is the phase angle measured in a coordinate system of the galaxy from the receding part of the major axis and  $V_{\text{exp}}$  is the expansion velocity of the galaxy (should be 0 in most cases).

Fitting is done iteratively with an additional parameter fixed in every new iteration - coordinates of the center ( $x_0, y_0$ ), systemic velocity ( $V_{\text{sys}}$ ), position angle (*P.A.*) and inclination ( $i$ ). Position angle and inclination were fixed to a series of values, so they would allow for presumed physical changes in these two parameters, for example due to warps. Adopted rotation curve and radial profiles for the position angle and inclination for the galaxy NGC 5055 are shown in Fig. 2 on the left (from Jovanović 2017).

How the rotation curve of the galaxy NGC 2366, based on our rotationally dominated velocity field, compares with ones based on Gauss-Hermite  $h_3$  and mean

<sup>1</sup>available at: <http://www.mpia.de/THINGS>.

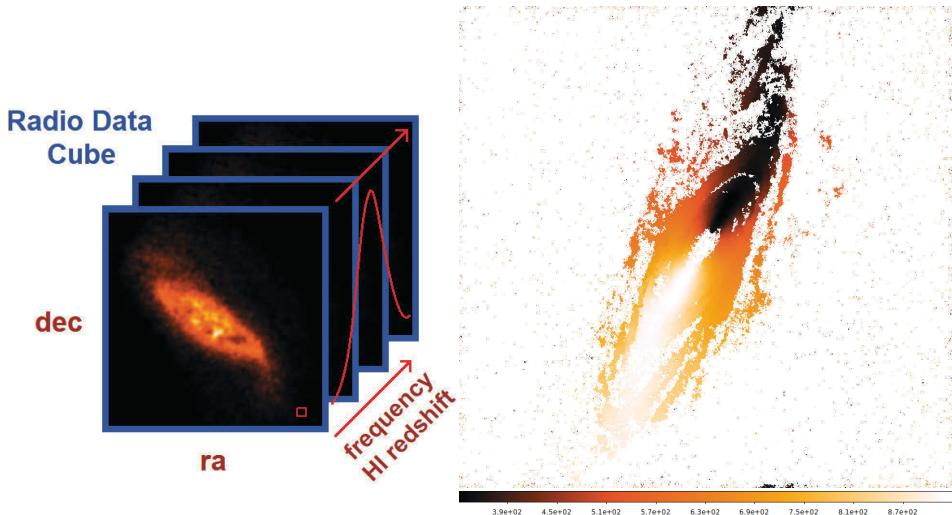


Figure 1: Left: The schematic of the three-dimensional HI observation i.e. data cube. At every pixel we fit the function or use similar procedure to find the center of the line. Right: Velocity field of NGC 2841 derived by using  $h_3$  polynomial.

intensity-weighted velocity (moment 1) is shown in Fig. 2 on the right. All the admitted points in the final rotation curve (blue stars in Fig. 2, right) were present in the observations and not extrapolated. By applying the developed procedure we were able to filter out the profiles that were probably affected by streaming and other non-rotational motions. This provided a rotation curve that is flat to a much larger radius (7.5 compared to 4.5 kpc).

### 3. 2. DYNAMICAL MODELING

We use the rotation curve to assess the whole enclosed gravitational mass of a galaxy and through dynamical modeling we compare this mass with known contributions from individual galaxy components like stars and gas.

Distances to galaxies in our sample are from the Extragalactic Distance Database<sup>2</sup> and they are mainly based on the Cosmicflows-3 results (Tully et al. 2016).

The gaseous component was also calculated from the THINGS data. Integrated intensity from HI radiation was used, scaled by a factor of 1.36 to account for other species of the cold neutral gas.

Stellar mass was assessed from its radiation by determining the mass-to-light ratio,  $M/L$ . This has been done in two different ways - by scaling the observed light with free parameter  $M/L$  and by assessing  $M/L$  from Stellar Population Synthesis (SPS) models.

For dynamical modeling with free  $M/L$  we use the Spitzer 3.6 micron observations to account for stellar light. SINGS<sup>3</sup> products and Spitzer Heritage Archive<sup>4</sup> images were used and then approximated with known models for stellar light like exponential

<sup>2</sup>Available at: <http://edd.ifa.hawaii.edu/>.

<sup>3</sup>Available at: <http://irsa.ipac.caltech.edu/data/SPITZER/SINGS>.

<sup>4</sup>Available at: <https://sha.ipac.caltech.edu/applications/Spitzer/SHA/>.

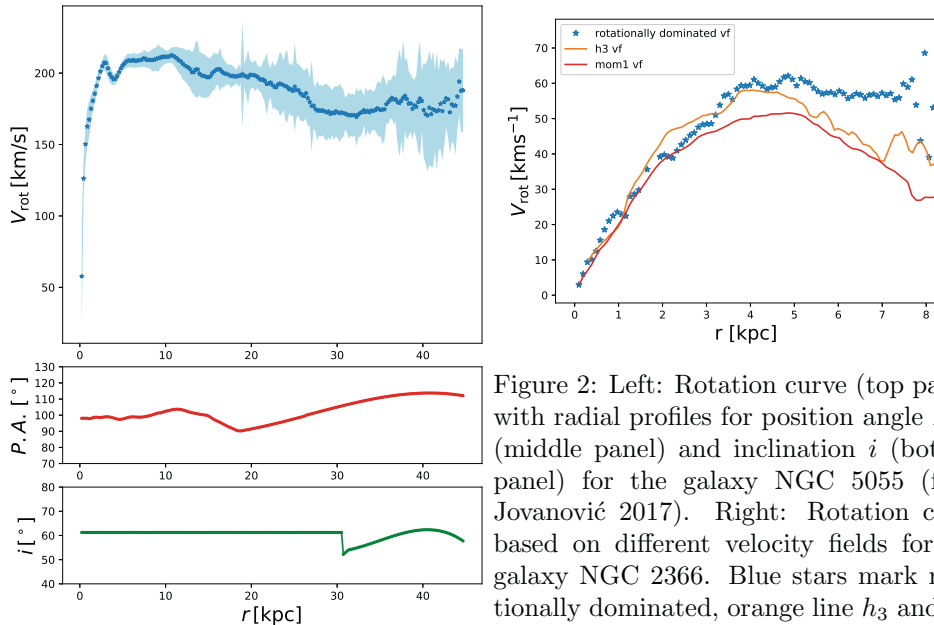


Figure 2: Left: Rotation curve (top panel) with radial profiles for position angle  $P.A.$  (middle panel) and inclination  $i$  (bottom panel) for the galaxy NGC 5055 (from Jovanović 2017). Right: Rotation curve based on different velocity fields for the galaxy NGC 2366. Blue stars mark rotationally dominated, orange line  $h_3$  and red line moment 1 velocity field.

disk or Sérsic bulge. Surface brightness models do not deviate significantly from the observed light distribution, so we can consider this component to be observationally based. The near-infrared  $3.6 \mu\text{m}$  band is thought to trace the old, most massive populations well and is subjected to less extinction. Part of the radiation in this band comes from the dust (Meidt et al. 2014, Querejeta et al. 2015), which is an issue that has not been addressed in our current work.

For SPS models different colors and metallicity (where possible) were used to calculate an M/L ratio using different evolutionary models - based on different initial mass function (IMFs), Star Formation History (SFH), stellar spectra, isochrones, etc. - 13 of them. Calculations of M/L are based on the evolutionary models compiled in Bell & de Jong 2003 and Into & Portinari 2013. It was possible to find a satisfactory dynamical model for 16 galaxies out of 20 (that were used with free models) when fixed M/L was used.

Two classical dark matter profiles were used - isothermal sphere (ISO, Jimenez et al. 2003) and Navarro-Frenk-White (NFW, Navarro, Frenk & White 1997). Originally THINGS data were intended for differentiating between core and cusp dark matter profiles that required sub-kpc scale.

For brevity, here we present an example of the dynamical models with free M/L (see Fig. 3) and isothermal dark matter halo for two galaxies - NGC 5055 and DDO 154 (published in Jovanović 2017).

Both galaxies have satisfactory dynamical models for free M/L and for NGC 5055 SPS models yield the M/L value in the 3.6 micron band that is compatible with the observed rotation curve. For DDO 154 majority of colors are outside the ranges covered with SPS models (which is sometimes the case with dwarf low-metallicity

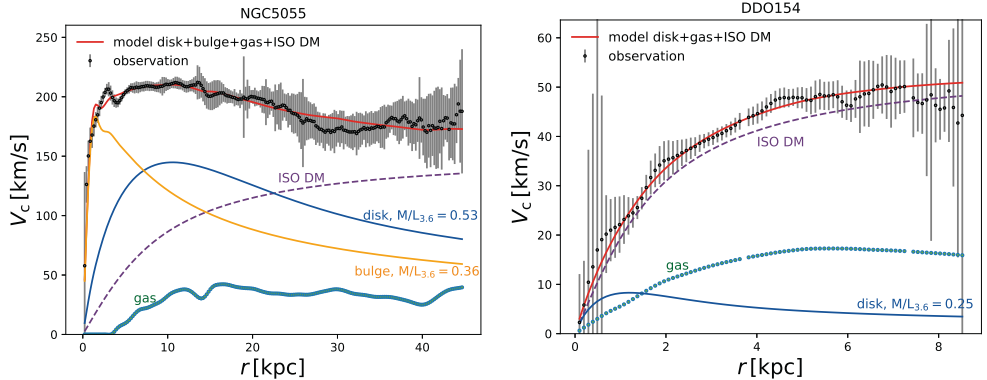


Figure 3: Fitting the observed rotation curves using free M/L and isothermal dark matter profile in case of NGC 5055 (left) and DDO 154 (right).

Table 1: Baryonic mass ( $M_{\text{baryon}}$ ) and baryonic fraction ( $\frac{M_{\text{baryon}}}{M_{\text{total}}}$ ) from dynamical models with free and fixed/SPS mass-to-light ratio and dark matter models (ISO and NFW) is given alongside the morphological type and distance in megaparsecs (from EDD, see footnote 2) for two galaxies from our sample, NGC 5055 and DDO 154.

Galaxy ID	morph. type	$D$ [Mpc]	$M/L$	dark matter model	$M_{\text{baryon}}$ [ $10^{10} M_{\odot}$ ]	$\frac{M_{\text{baryon}}}{M_{\text{total}}}$
NGC 5055	Sbc	$8.99 \pm 0.45$	free	ISO	$13.3 \pm 0.6$	$0.42 \pm 0.25$
				NFW	$12.1 \pm 0.7$	$0.38 \pm 0.09$
			SPS	ISO	$11.2 \pm 4.0$	$0.37 \pm 0.80$
				NFW	$10.9 \pm 3.9$	$0.4 \pm 1.7$
DDO 154	I	$4.04 \pm 0.20$	free	ISO	$0.53 \pm 0.02$	$0.10 \pm 0.03$
				NFW	$0.53 \pm 0.01$	$0.10 \pm 0.01$
			SPS	ISO	$0.52 \pm 0.01$	$0.09 \pm 0.01$
				NFW	$0.52 \pm 0.01$	$0.09 \pm 0.01$

galaxies). Still, several models do give credible values of M/L that we were able to use in dynamical modeling. Previously observed difficulties of NFW to successfully fit the rotation curves of dwarf galaxies in the center (for example DDO 154) are noted in our work as well.

For all 20 galaxies we calculated the enclosed masses of all the considered components up to the outermost observed radii, and they include the mass of the gas, stellar components, dark matter halo (this is the only component that can actually be extrapolated given that its density profile is theoretical), total mass and baryonic mass. Our primary interest is baryonic mass function (BMF), which is the distribution of baryonic mass (regular mass consisting of protons and neutrons) in our sample. An example of the baryonic mass and fraction calculated from dynamical models for

galaxies NGC 5055 and DDO 154 is given in Table 1. The outline of baryonic mass distribution for models with free M/L and isothermal dark matter is shown in Fig. 4.

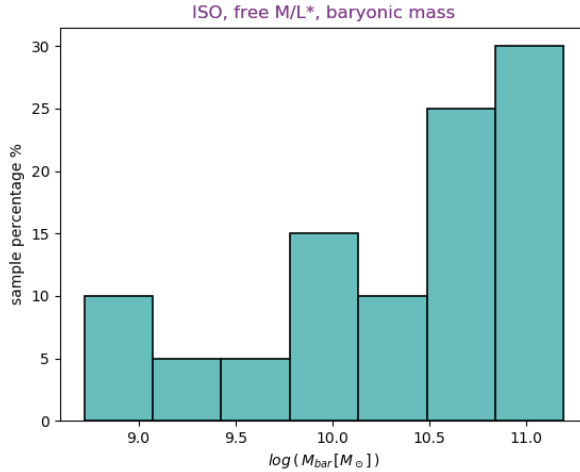


Figure 4: Distribution of the baryonic mass in THINGS galaxies based on dynamical models using free M/L ratio and isothermal dark matter profile.

Detailed analysis of the dynamical models for all the galaxies in the sample along with the discussion are a subject of the PhD thesis of M. Jovanović and a publication in preparation.

### Acknowledgements

This work was supported by the Ministry of Education, Science and Technological Development of the Republic of Serbia (MESTDRS) through the contract No. 451-03-68/2020-14/200002. Useful discussions with Dr. M. Bílek and Dr. M. Jurkovic are acknowledged.

### References

- Bell E. F., de Jong R. S.: 2001, *ApJ*, **550**, 212.  
 Courteau, S., Cappellari, M., de Jong, R. S. et al.: 2014, *Rev. Mod. Phys.*, **86**, 47.  
 de Blok, W. J. G., Walter, F., Brinks, E., Trachternach, C., Oh, S.-H., Kennicutt, R. C., Jr: 2008, *AJ*, **136**, 2648.  
 Into, T., Portinari, L.: 2013, *MNRAS*, **430**, 2715.  
 Jimenez, R., Verde, L., Treu, T., Stern, D.: 2003, *ApJ*, **593**, 622.  
 Jovanović, M.: 2017, *MNRAS*, **469**, 3564.  
 Meidt, S. E., Schinnerer, E., van de Ven, G. et al.: 2014, *ApJ*, **788**, 144.  
 Navarro, J. F., Frenk, C. S., White, S. D. M.: 1997, *ApJ*, **490**, 493.  
 Oh, S.-H., de Blok, W. J. G., Brinks, E., Walter, F., Kennicutt, R. C., Jr: 2011, *AJ*, **141**, 193.  
 Querejeta, M., Meidt, S. E., Schinnerer, E. et al.: 2015, *ApJS*, **219**, 5.  
 Samurović, S., Vudragović, A., Jovanović, M.: 2015, *MNRAS*, **451**, 4073.  
 Tully, R. B., Courtois, H. M., Sorce, J. G.: 2016, *AJ*, **152**, 50.  
 Walter, F., Brinks, E., de Blok, W. J. G., Bigiel, F., Kennicutt, R. C., Jr, Thornley, M. D., Leroy, A.: 2008, *AJ*, **136**, 2563.